PROCEEDINGS OF SCIENCE

Investigating the degradation effects of wall-paintings under a compartment fire protocol

Lamprini Malletzidou*, Triantafillia Zorba, Konstantinos Chrissafis, George Vourlias and Konstantinos M. Paraskevopoulos

Laboratory of Advanced Materials & Devices, School of Physics, Faculty of Sciences, Aristotle University of Thessaloniki
Thessaloniki, GR-54124, Greece

E-mail: labrinim@auth.gr, zorba@auth.gr, hrisafis@physics.auth.gr, gvourlia@auth.gr, kpar@auth.gr

The presence of binding media is considered as one of the criteria towards the identification of the technique that was employed for the completion of a wall painting. Following this, the degradation of binding media during a natural disaster is of great importance, not only for the integrity of the artifact, but also for the identification of the applied technique. Fire belongs to such disastrous events, that can be catastrophic to every artifact. In the case of wall paintings, these effects vary from surface depositions to their total collapse, always in accordance with the maximum temperature and the duration of the incident. In the framework of a first approximation step towards understanding the effects of fire, or the maximum temperatures developed over the painting layers of wall paintings, the present study is focused on the preparation of mock-ups following traditional wall painting recipes. In every case, commercially available yellow ochre was used as the pigment under study, while the painting layers were applied following the *fresco* and *secco* techniques; for the latter, egg yolk, linseed oil, gum Arabic and casein were used as the binding media. The wall painting mock-ups -and the pigment separately- both underwent an annealing protocol, representative of compartment fires. The pigment alone was studied by means of thermogravimetry (TGA), Fourier transform infrared spectroscopy (FTIR) and X-rays diffractometry (XRD), while the ground of the mock-ups was examined with FTIR and TGA, and the painting layers were observed and studied using UV-Vis spectrophotometry, towards the understanding of their macroscopic and morphological alterations.

11th International Conference of the Balkan Physical Union (BPU11),
28 August - 1 September 2022
Belgrade, Serbia

* Speaker

PoS(BPU11)132

1. Introduction

Fires in general are regarded as extreme and disastrous incidents in every case, that can be caused from accidents, war events, or even vandalism and terrorism. Especially in the case of monuments bearing painted surfaces, fires that take place in the interior of a construction can result to various conditions, from aesthetic problems (smoke blackening), up to minor and major results, such as micro-cracks, instability of painting layers, color changes, defacement caused of the binder or the plaster deterioration and even structural instabilities, up to the extremity of even the partial or whole collapse of the monument. According to existing literature regarding thermal aging or fire alterations, fire damages are considered as irreversible damages to monuments, as their affects compromise even the most rigid materials, i.e. the building materials of the monuments, causing cracks and porosity changes. These effects can accumulate to lead to even the full collapse of the building [1,2].

The course of a fire into a compartment is usually characterized by the following steps [3,4]:

(a) Ignition, which is considered as the initial step/beginning of a fire,
(b) Growth, when the fire keeps developing as a function of its initial fuel, without influencing the compartment. As a result, this stage is characterized by low temperatures into the compartment itself and material failure is negligible. If the fire is supported by surrounding fuel and oxygen, it will grow causing high temperatures in the compartment.
(c) Flashover; this stage involves all the combustible materials in the compartment, causing their ignition.
(d) Full development, where temperature rises until a certain value with a maximum of heat release.
(e) Decay, when all fuels are consumed.

These steps are also described by the temperature-time curves of fires, although several fire parameters are unpredictable or vary in each case, such as the amount and the surface area of the combustible materials, air ventilation etc., which can lead to various temperature courses with equal probability [3]. These parameters have been studied in the case of compartment fires, although the term “compartment fires” refers to fires that develop in enclosed buildings of less than 100 m^2 [5].

The three usual methods for the study of fire effects are (a) modeling of fire temperatures in ovens (lacking air circulation stimulation and combustion), (b) the use of real flames (uncontrollable and with random results) and (c) laser burning simulating temperature effects and heating reactions [2]. Until now, the literature regarding the fire effects on monuments is mostly focusing on construction materials [6–8]. In existing literature [9,10], regarding the study of stones damaged by fire, a fire-approaching protocol was used, where the samples were annealed up to a maximum temperature (T_{max}), with a heating rate of T_{max}/h, and kept there for 6 hours. Although this annealing protocol is not exactly depicting a natural fire [9], it is quite representative of fire temperatures and duration, according to temperature/time curves as presented by Sundström and Gustavsson [11], and Walton and Thomas [4]. A differentiated protocol was applied by Dionísio et al. [12] but in the same direction, as the heating rate was kept half (30 min for T_{max} instead for an hour), and the annealing at T_{max} had a duration of 24 h. In a recent review paper [13], the authors gathered together -among others- all the annealing protocols applied to study fire effects on stone materials.

Regarding the painting layers of wall paintings, they consist of a plethora of materials, both of organic and inorganic nature, directly depending on the wall painting technique that was used by the artists themselves. Following the two major wall painting techniques -*a fresco* and *a secco*- in the first, the painting layers are applied mixed with plain water; the mechanism of calcium carbonate formation from the fresh lime ground results to the incorporation of the pigment grains into the surface of the plaster layer. No other binding medium is needed for the stabilization of the painting layer. According to the *secco* technique, the painting layers are applied on dry ground, or even directly upon the masonry [14]. In this case, the painting layers consist of the pigment (or dye) used, mixed with an organic or even an inorganic binder (lime wash) [15]. Thus -and among other characteristics- the presence (or absence) of binding media is considered as one of the criteria for wall painting technique identification [15]. A detailed review presented by Casadio et al. is dealing with the organic materials that have been used as binders in wall paintings, according to surviving literature [16]. Apart from egg yolk and gum Arabic, usual organic binders used in *secco* painting are oils (with linseed oil being the most common), casein, wax, egg white, whole egg and milk.

In association with the most preeminent subject of wall paintings studies -which is the determination of the painting technique-, the following questions have arisen:

- After which annealing temperature are the presumable-to-be-used organic binders not detected?
- Can binders be detected after a fire incident, thus preserving indications regarding the applied painting technique?
- Can pigments, binders and plasters act as indicators regarding the maximum temperature developed during a fire incident?

As a first approximation step towards replying these questions, and as the subject of the present work, wall painting mock-ups bearing a yellow ochre painting layer were prepared according to the most usual wall painting techniques. After being subjected to an annealing protocol resembling compartment fires, the pigment and the mock-ups were studied, towards the recording of their macroscopic, morphological and structural alterations.

2. Experimental section

2.1. Preparation of wall-painting mock-ups

The wall painting mock-ups were prepared according to traditional recipes, but preserving their simplicity to a certain degree. Thus, the ground layer was prepared by $Ca(OH)_2$ (Chem-Lab NV, >95%, CL00.0321.1000), mixed with distilled water, without the use of aggregates that are common in plaster layers, i.e. sand. Immediately after its preparation, the plaster slurry was inserted into wooden molds; An hour after that, the molds were carved into smaller mock-ups of about (1.5 × 1.5) cm.

For the application of the painting layer, the same pigment was used in all the cases under study. Yellow ochre was chosen for this step, because it has a well-known behavior during annealing, as it is presented in the following. For this reason, commercial yellow “French Ochre JTCLES” by Kremer, with an order number of 4001, was used. The up-to-date info regarding the pigment (with an updated order number of 40010), describes it as a clear yellow earth pigment, washed, natural, from France, with a composition of $Fe_2O_3 + SiO_2 + Al_2O_3$ [17]. A second mock-

up series was prepared using cinnabar, but its study has been postponed due to the pigment's toxicity under annealing; this study is not a subject of the present work

The preparation of the painting media that were used for the painting layers of the mock-ups is described in Table 1. The media were mixed with the pigment under study in order to form pastes, which were then applied on the mock-ups using separate paintbrushes, to avoid cross-contamination between the organic binders.

Fresco	
The pigment was mixed with distilled water and the painting layer was applied after 2 h of plaster preparation	
Secco	
The pigment was mixed with the following media. The painting layers were applied after 48 h of plaster preparation	
Egg yolk	The yolk of a commercially available fresh egg was used, after it was extracted from the vitelline membrane with a sterile syringe. As a next step, some drops of distilled water were added
Linseed oil	Commercially available stand oil by ROYAL TALENS was used
Gum Arabic	A piece of gum Arabic (63300, Kremer) was left for 24 hours in a shield glass container with warm distilled water to be dissolved (1 part gum per 2 parts of water). The liquid was then mixed with the pigment in order to obtain a paste
Casein	75 g of casein powder (63200, Kremer) were soaked in 125 ml of distilled water over night

Table 1: *The recipes followed for the preparation and application of the painting layers of the mock-ups.*

Finally, all the mock-ups were left to dry/"naturally age" in room conditions for 9 months, before the annealing protocol was performed (Fig. 1). The exact time period of the characterization measurements will be mentioned in the following paragraphs, for each method separately.

Figure 1: *The mock-ups prepared under different wall painting techniques. Vermillion was used for the ones of red color, but because of their toxicity during annealing, their study was postponed.*

2.2. Annealing procedure

After a time period of 9 months, during which the wall painting mock-ups were left to naturally age, they were subjected to the annealing protocol as described in the following. The heating treatment took place in a high-temperatures continuous programmable oven (Nabertherm GMBH, type HTC 03/16, with control panel P320). Groups of the wall painting mock-ups -every group contained one mock-up from each painting method- were inserted into the oven, placed on an alumina board. A quantity of the yellow ochre under study, placed in a porcelain crucible, was also heat-treated together with the mock-ups at every heating temperature.

The upper heating limit was set to 700 °C, as the plaster mock-ups are composed of $CaCO_3$; the degradation of carbonaceous materials at around this temperature [18] is indeed our upper limit, as above this the plaster, and consequently a wall painting, starts to fall apart. On the other hand, traditional plaster recipes include sand. Although sand was not incorporated in the plaster preparation -in order to keep it as simple as possible- it is worth to mention that quartz transforms from α- to β- at about 550 °C -increasing in volume- [9,18], which also contributes to the development of mechanical stress inside the plaster, and in the painting layers (especially regarding pigments containing quartz). This fact can act also as a limit above which a wall painting starts to fall apart.

Different groups of the wall painting mock-ups -together with separate amounts of the pigment under study- were heated in the oven at maximum temperatures (T_{max}) of 100, 200, 250, 300, 350, 400, 450, 500, 600 and 700 °C. In every case, the applied temperature reached its maximum in 60 minutes (heating rate of T_{max}/h). As a next step, the specimens remained for 6 hours at T_{max}, and then left to cool down slowly inside the oven [9,10]. All the specimens were kept into containers afterwards, until their characterization study.

2.3. Characterization techniques

Fourier transform infrared spectroscopy (FTIR) measurements were performed using two different spectrometers and measurement modes, due to infrastructure availability during the long time period between the measurements. The plaster layer of the mock-ups after 3 years of its preparation and without being subjected to the annealing procedure (Fig. 2a) and yellow ochre (Fig. 3a) were analyzed using a Spectrum 1000 Perkin-Elmer FTIR spectrometer in transmittance mode, in the spectral area 4000-400 cm^{-1}, with a resolution of 4 cm^{-1} and 64 consecutively collected scans, using the KBr pellet technique. On the other hand, the plaster layer of the mock-ups, naturally aged for 5 years after their preparation, was examined with a Cary 670 Agilent FTIR spectrometer, in attenuated total reflectance (ATR) mode, under the same measurement conditions, using a diamond ATR apparatus, GladiATR PIKE. For comparative reasons, the ATR-FTIR spectrum was transformed to transmittance (Fig. 2a).

XRD measurements were applied to the pigment under study, in order to identify all the phases present before and after the application of the annealing protocol. The pigment specimens were stored in a desiccator, in sealed Eppendorf containers, immediately after the annealing protocol, in order to postpone any air results, i.e. the formation of $CaCO_3$, because of humidity and atmospheric CO_2. The specimens were studied with a two-cycle Rigaku Ultima$^+$ X-ray diffractometer (40 kV/30 mA, CuK_α radiation, Bragg-Brentano geometry). The collected XRD patterns were identified with the PDF cards: Calcite hexagonal #47-1743, quartz hexagonal #46-

1045, kaolinite monoclinic #29-1488, goethite orthorhombic #81-0464, hematite hexagonal #79-0007, and lime (CaO) cubic #48-1467 [19].

Thermogravimetric analysis (TGA) was performed with a Setsys 16/18 Setaram TG-TDA instrument. The samples of mass (10 ± 0.5) mg were placed in alumina crucibles for the measurements, where an empty alumina crucible was used as the reference. The samples were heated from ambient temperature up to 1100 °C, and a heating rate of 20 °C/min was applied, with air flow of 50 ml/min. Before each measurement, the same conditions were applied for each empty crucible, in order to be used as the background measurement.

UV-Vis spectrophotometry was performed with a Lambda 18 Perkin-Elmer spectrometer, equipped with an integrating sphere covered with $BaSO_4$. The measurements were performed in diffuse reflectance mode, in the spectral region of 200-800 nm, with a tungsten-halogen lamp (320-800 nm) and a deuterium lamp (200-320 nm), with automatic source change at 320 nm, with a step of 1 nm, and 4 scans for each measurement. A freshly pressed $BaSO_4$ background was used for the autozeroing of the measurements. The measurements were performed on the painting surface of the samples that maintained their integrity after the annealing process. For this reason, the method was not applied to samples annealed at temperatures that exceeded 500 °C, as above this temperature the plaster layer collapsed, resulting to fragments smaller than the spectrometer's sample window. The collected spectra were further manipulated to acquire their colorimetric parameters according to CIE 1976 $L^*a^*b^*$ (henceforth CIELab) standards [20]. According to CIELab color space, L^* presents the lightness, a^* and b^* the color coordinates, C^*_{ab} the chroma (as presented in Eq.1) and ΔE^*_{ab} the color difference (as presented in Eq. 5), and hue difference (ΔH^*) is calculated as in Eq. 6:

$$C^*_{ab} = (a^{*2} + b^{*2})^{1/2} \quad \text{Eq. 1}$$

$$\Delta a^* = a^*_f - a^*_i \quad \text{Eq. 2}$$

$$\Delta b^* = b^*_f - b^*_i \quad \text{Eq. 3}$$

$$\Delta L^* = L^*_f - L^*_i \quad \text{Eq. 4}$$

$$\Delta E^* = \left[\Delta L^{*2} + \Delta a^{*2} + \Delta b^{*2}\right]^{1/2} \quad \text{Eq. 5}$$

$$\Delta H^* = \left[\Delta E^{*2} - \Delta L^{*2} - \Delta C^{*2}\right]^{1/2} \quad \text{Eq. 6}$$

In every case, the *"f"* indicates the final state of the sample under investigation, i.e. the annealed mock-up to each T_{max}, while *"i"* indicates their initial state, before the annealing.

3. Results and Discussion

3.1. Plaster layer analysis

Figure 2 shows the FTIR and TGA analyses performed to the mock-ups' plaster. The FTIR spectra, collected after 3 and 5 years from its preparation (Fig. 2a) still present the band at 3644 cm^{-1}, which is attributed to $Ca(OH)_2$. This shows that the carbonation process is slow. On the other hand, apart from the characteristic bands of calcite at 873 and 712 cm^{-1}, the phase of aragonite is also present, because of its characteristic bands at 1078, 856 and 700 (shoulder) cm^{-1}. Considering the fact that the existence of aragonite has been previously observed together with calcite, during the carbonation of $Ca(OH)_2$ [21], this finding is very interesting as it seems that during this process, both carbonate phases occur, at least before the domination of calcite, as aragonite is

unstable at ambient conditions [22–24]. Studies have shown that the carbonation process of $Ca(OH)_2$ in biomaterials is described by the following sequence:

$$Ca(OH)_2 \rightarrow hydrated\ ACC \rightarrow ACC \rightarrow vaterite \rightarrow aragonite \rightarrow calcite \quad \text{Eq. 7}$$

where ACC is amorphous calcium carbonate ([25] and references within). The formation of vaterite and aragonite has not been identified in lime painting without the presence of Mg [25], in contradiction to the present experiment regarding the plaster.

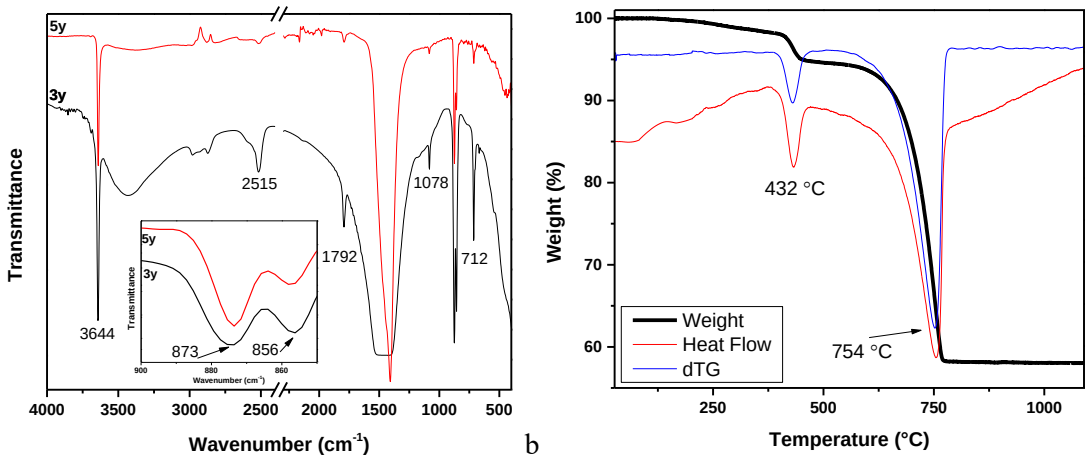

Figure 2: *FTIR spectra collected from a period of 3 & 5 years after their preparation (a), and thermogravimetric curves of weight, its first derivative (dTG) and heat flow (b) of the ground layer collected from the mock-ups under study 3 years after their preparation.*

The performed thermogravimetric analysis to the plaster of the mock-ups after 3 years after their preparation is presented in Fig. 2b. The first weight loss step, with a loss rate maximum at 432 °C, confirms the presence of $Ca(OH)_2$, as it is attributed to its dehydroxylation at 480 – 620 °C, with a mass loss of 9.3%, according to the reaction:

$$Ca(OH)_2 \rightarrow CaO + H_2O \quad \text{Eq. 8}$$

The second -and major- weight loss above 550 °C, with a maximum weight loss rate at 754 °C, is attributed to the decomposition of carbonates, according to the reaction:

$$CaCO_3 \xrightarrow{754\,^{\circ}C} CaO + CO_2 \uparrow \quad \text{Eq. 9}$$

It is observed that TGA confirms the presence of $Ca(OH)_2$, while the decomposition of the carbonate content follows that of literature regarding their maximum in weight loss rate [18].

3.2. Pigment analysis

The FTIR spectrum of the pigment under study is presented in Fig. 3a. It consists of kaolinite, goethite and calcite, because of the following characteristic bands:

- Goethite (FeOOH): 3145, 910, 796, and 468 cm^{-1} [26,27].
- Kaolinite ($Al_2Si_2O_5(OH)_4$): 3693, 3620,1090, 1032, 1006, 914, 792, 753, 696, 642, 600, 536, 470 and 429 cm^{-1} [26,28].
- Calcite ($CaCO_3$): 2873, 2512, 1797, 1429, 875 and 712 cm^{-1} [29,30].

At this point, it is worth to mention that the participation of calcite is not stated in this specific pigment's composition [17]. Furthermore, lepidocrocite, another iron hydroxy oxide often being

present in natural yellow ochres, with characteristic FTIR bands at 3120, 1157, 1020, 746, 515, 478 cm^{-1}, has not been detected.

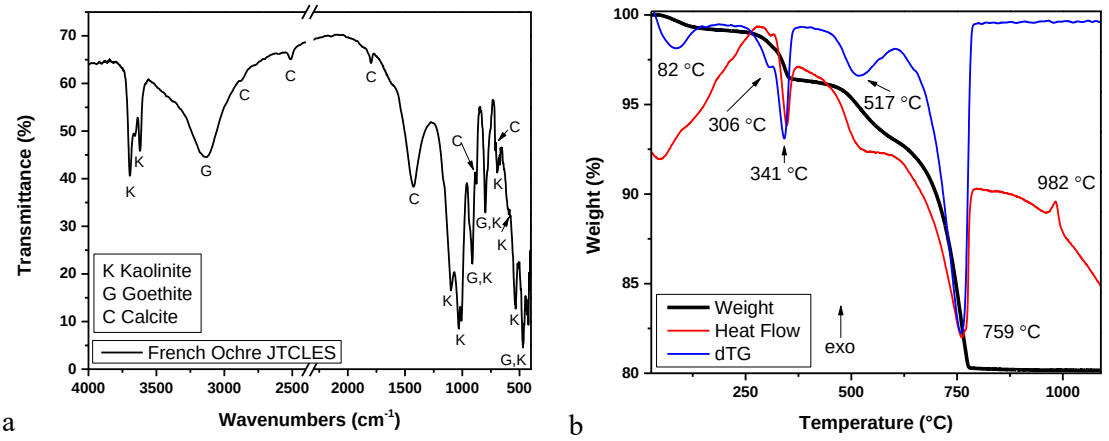

***Figure 3**: FTIR spectrum (a) and thermogravimetric curves of weight, its first derivative (dTG) and heat flow (b) of the pigment under study (yellow French Ochre JTCLES, 4001, Kremer).*

The thermographs of yellow ochre are presented in Fig. 3b. The first weight loss which ends at ~150 °C, with a maximum in the loss rate at 82 °C, is attributed to moisture. Iron hydroxyl-oxide dehydroxylates at with a maximum in loss rate at 341 °C in the case of goethite (α-FeOOH), and at about 306 °C in the case of lepidocrocite (γ-FeOOH), according to the reactions:

$$2\alpha - FeOOH \xrightarrow{341\,^{\circ}C} \alpha - Fe_2O_3 + H_2O \uparrow \quad \text{Eq. 10}$$

$$2\gamma - FeOOH \xrightarrow{306\,^{\circ}C} \gamma - Fe_2O_3 + H_2O \uparrow \xrightarrow{400\,^{\circ}C} \alpha - Fe_2O_3 \quad \text{Eq. 11}$$

where maghemite (γ-Fe_2O_3) transforms to hematite (α-Fe_2O_3) with an exothermic reaction at 400 °C. Kaolinite dehydroxylates at 530 – 590 °C, resulting into amorphous meta-kaolinite, while it transforms into other crystalline phases with an exothermic peak at 982 °C, according to the reactions [18]:

$$Al_2Si_2O_5(OH)_4 \xrightarrow{517\,^{\circ}C} Al_2O_3 \cdot 2SiO_2 + H_2O \uparrow \quad \text{Eq. 12}$$

$$3(Al_2O_3 \cdot 2SiO_2) \xrightarrow{982\,^{\circ}C} 2Al_2O_3 \cdot 3SiO_2 + 3SiO_2 + \gamma Al_2O_3 \quad \text{Eq. 13}$$

The highest weight loss with a maximum of the weight loss rate at 759 °C is attributed to the decomposition of calcite, according to the reaction presented in Eq. 9 [18,21,31]. In general, TGA analysis of yellow ochre presents the same characteristics as discussed by Thomas et al. [32]. It should be noted that through TGA, the presence of lepidocrocite was confirmed.

In Fig. 4, representative XRD diffraction patterns of the pigment under study are presented, unheated and after the annealing protocol. The unheated pattern shows that the pigment mainly consists of kaolinite, calcite, goethite and quartz. Additionally, some peaks of low intensity (e.g. the peak at 8.85°) could be attributed to minor aluminosilicate phases containing iron, such as muscovite. Following the temperature increase according to the annealing protocol, it is noted:

- 100 - 250 °C: No differentiation is observed, except from a slight variation of the kaolinite's diffraction peaks intensities, which can be attributed to homogeneity variations of the pigment.
- 300 °C: Goethite diffraction peaks disappear; Hematite peaks are noticed.
- 400 °C: Small decrease in the diffraction peaks of kaolinite.
- 500 °C: Dramatical reduction of kaolinite, no indication of metakaolinite's formation, which is attributed to its amorphous state [33].

- 600 °C: Beginning of calcite's diffraction peaks reduction.
- 700 °C: Quartz, hematite and CaO are the identified components.

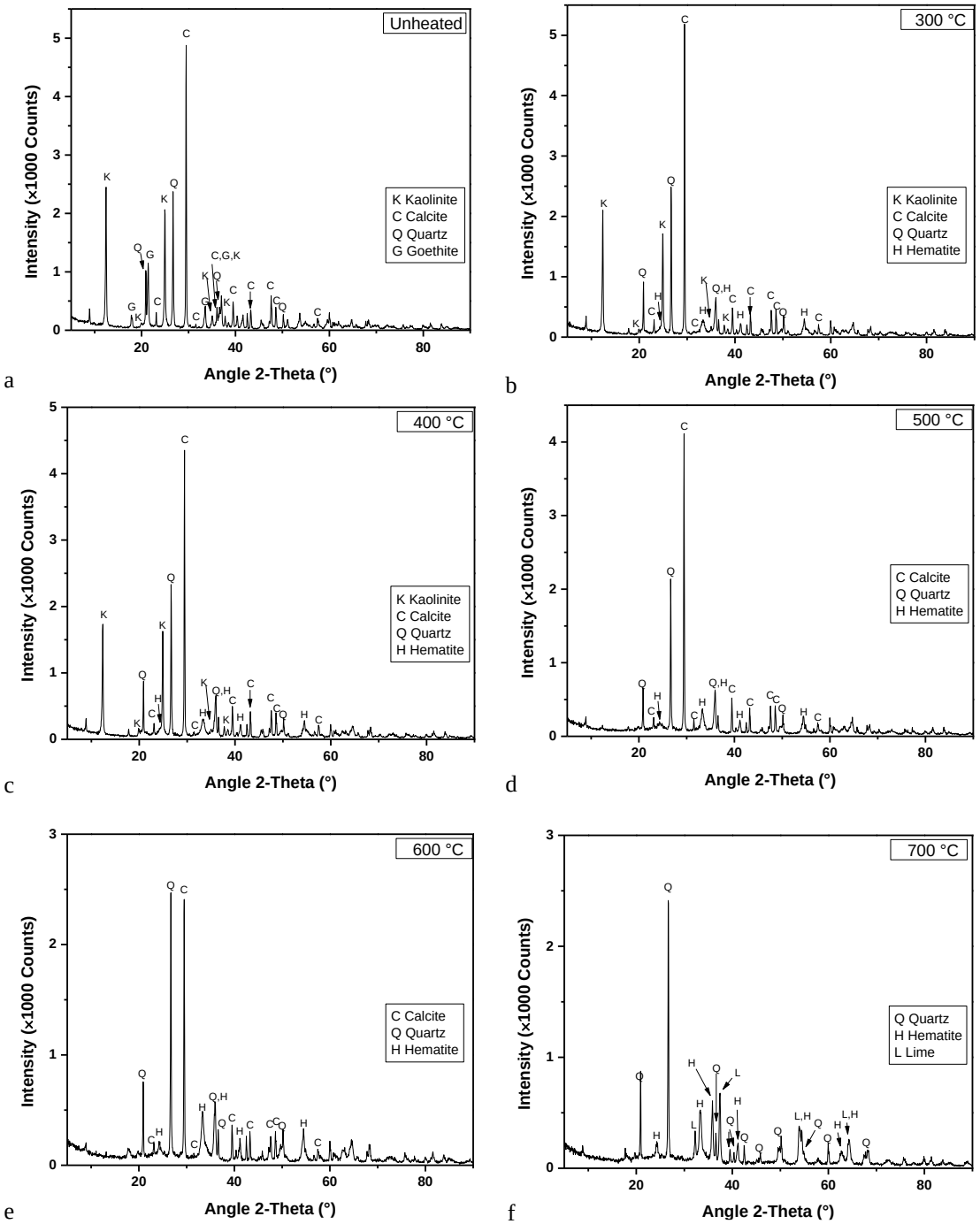

Figure 4: *XRD diffraction patterns of yellow ochre after the annealing protocol.*

Regarding the low intensity of goethite peaks in the pattern of the pigment as received (Fig. 4a), the Rietveld analysis that was performed using the open-source FullProf Suite program (version January-2021), showed a relatively low participation of 10.2% in goethite, while the other identified components -quartz, kaolinite and calcite- presented a weight quantification of 13.3, 37.1, and 39.5%, respectively.

Comparing the characterization results of FeOOH with the three applied techniques (FTIR, XRD and TGA), the following are noted. Natural ferrous pigments, such as ochre, usually exist in mixtures with aluminosilicates, such as kaolin-type minerals, and other minerals and oxides, such as calcite, quartz, gypsum, TiO_2 etc. [34–36]. Goethite is clearly identified through XRD analysis, together with calcite, kaolinite and quartz, while these findings are in agreement with FTIR analysis. On the other hand, it should be noted that most of the characteristic FTIR bands of FeOOH are strongly overlapped from those of the other components of the pigment under study, especially kaolinite. Considering the fact that painting layers are even more complicated mixtures, as they can consist of organic materials -in the case of binding media-, and inorganics -i.e. other pigments-, the need of applying a combination of characterization methods for the certain identification of yellow ochre is noticeable. In this direction, TGA analysis is a promising technique in the study of this particular pigment under examination, as both forms of FeOOH (α-FeOOH, and γ-FeOOH) were identified.

3.3. Macroscopic characteristics

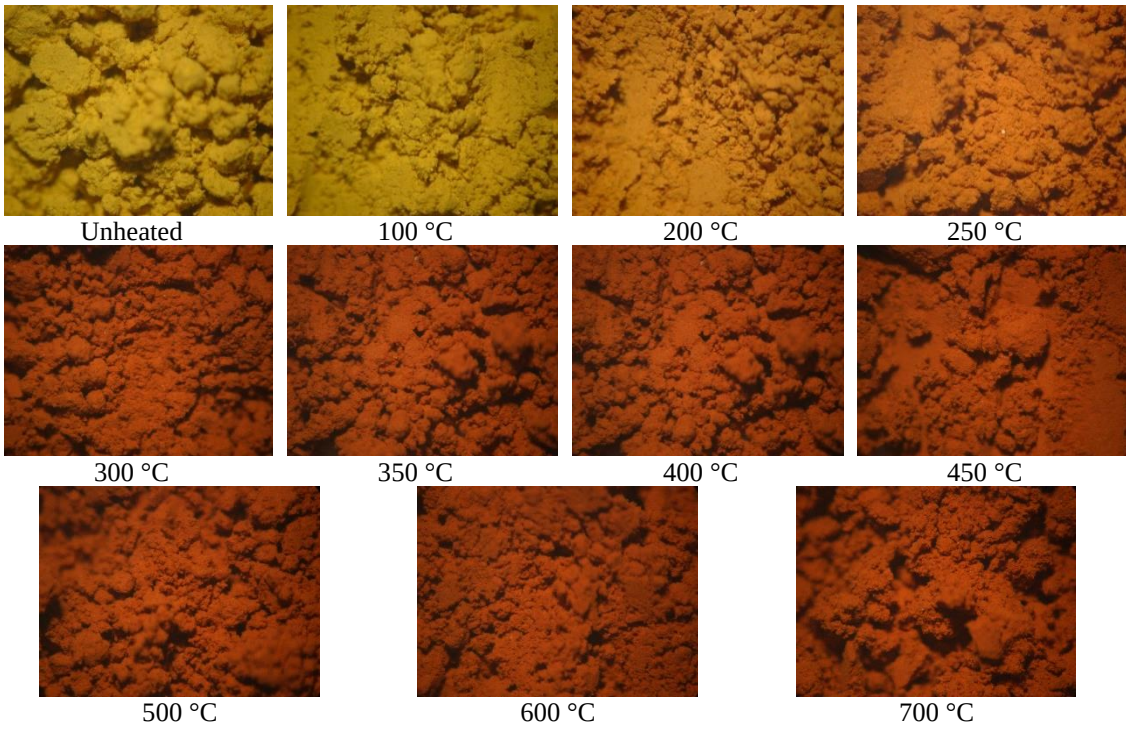

***Figure 5**: Optical microscopy images from yellow ochre, unheated and after the annealing protocol.*

Figures 5 and 6 present the optical images of the pigment and the mock-ups, respectively, unheated and after the annealing protocol. Regarding the painting layer of the mock-ups, their yellow color remains intact up to T_{max} = 200 °C. A small alteration appears at T_{max} = 250 & 300 °C, where ochre presents an orange and a brown hue, respectively. For $T_{max} \geq 350$ °C, the painting layer achieves a dark red/brown color. In the case of the neat pigment itself, as presented in Fig. 5, the color alteration begins at T_{max} = 200 °C, turning to a somewhat warmer hue. Apart from that, the rest of the changes follow that of the painting layer of the wall painting mock-ups.

Regarding their stability, macroscopic cracks start to appear at T_{max} = 400 °C, more severe cracks at 500 °C, where the mock-ups presented splits, while at $T_{max} \geq 600$ °C the mock-ups

almost totally collapsed, as they turned into small fragments. This is in agreement with Hajpál and Török [9], as the authors reported textural damages in sandstones containing calcite, from 450 °C and above.

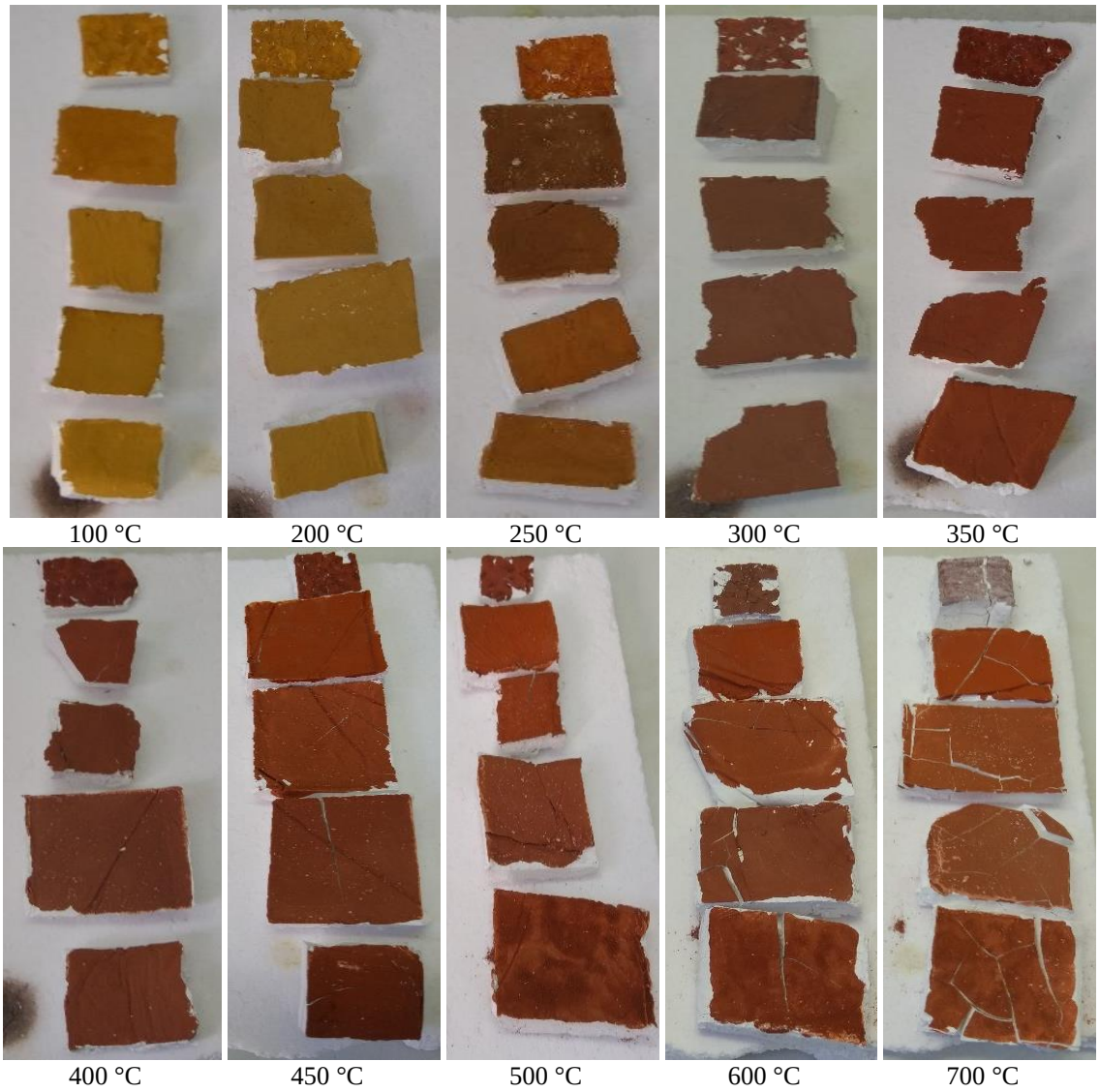

Figure 6: *Optical images from the wall painting mock-ups under examination, unheated and after their annealing according to the applied protocol (top to bottom: fresco, egg yolk, linseed oil, gum Arabic and casein).*

3.4. UV-Vis Spectrophotometry

The measurements were performed on the painting surface of the samples and only to samples that maintained their integrity after the annealing process. For this reason, the method was not applied to samples annealed at temperatures that exceeded 500 °C, as above this temperature the plaster layer collapses, resulting to fragments smaller than the spectrometer's sample window.

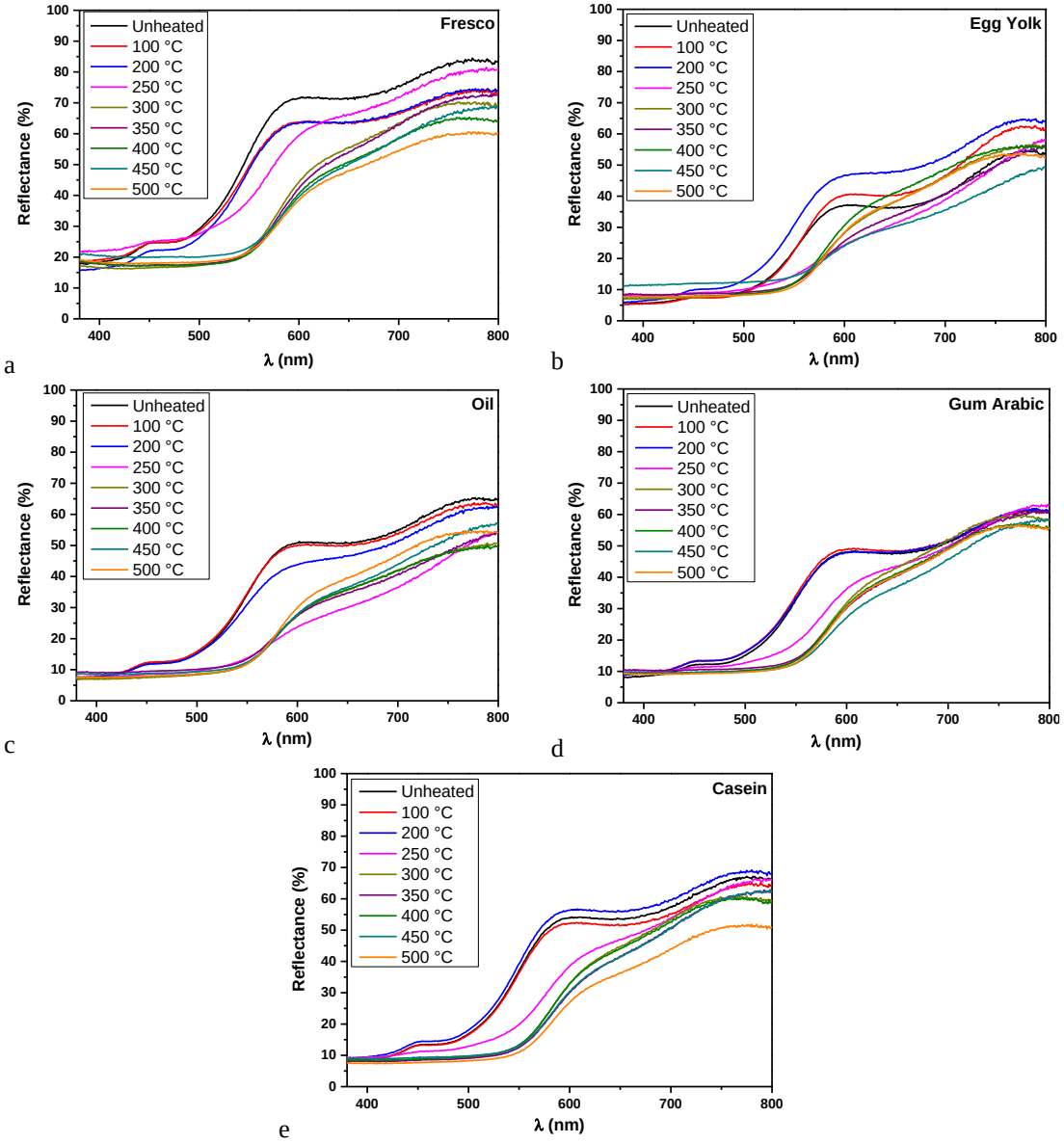

***Figure 7**: Diffuse reflectance spectra of all the mock-ups under study.*

The diffuse reflectance spectra of the mock-ups under study are presented in Fig. 7. In general, the spectra collected of each binder-series are classified in two distinctive groups. In the first group, all the spectra are included, that were collected from the mock-ups before heating and after annealed up to 200 °C. This group presents a distinctive and wide reflectance peak below 600 nm, which is characteristic of the yellow color of the pigment. The second group is characterized by the fact that this peak shifts to higher wavelengths when the mock-ups are being heated to higher temperatures, justifying their orange to brownish and then to red color transition, as also detected by optical observation. The higher reflectance of the fresco mock-ups is also noted. It is attributed to the thinner painting layer, resulting to the higher participation of the plaster reflectivity.

In Fig. 8, the results of the diffuse reflectance spectra of Fig. 7 are presented by means of the CIELab color coordinates differences, calculated with Eqs 1-6. All the mock-ups present their highest differentiation after their annealing at T_{max} of 250 °C, in accordance to their optical

observation, which is also depicted by the overall color difference (ΔE^*). In particular, color coordinate a^* shifts to higher values depicting the change of color to red, b^* shifts to lower values showing the lack of yellow, while their L^* values shift to lower values, showing their change to darker hue. Apart from that, the irregularities of the mock-ups with egg yolk as the binder are attributed to inconsistencies in the painting layer.

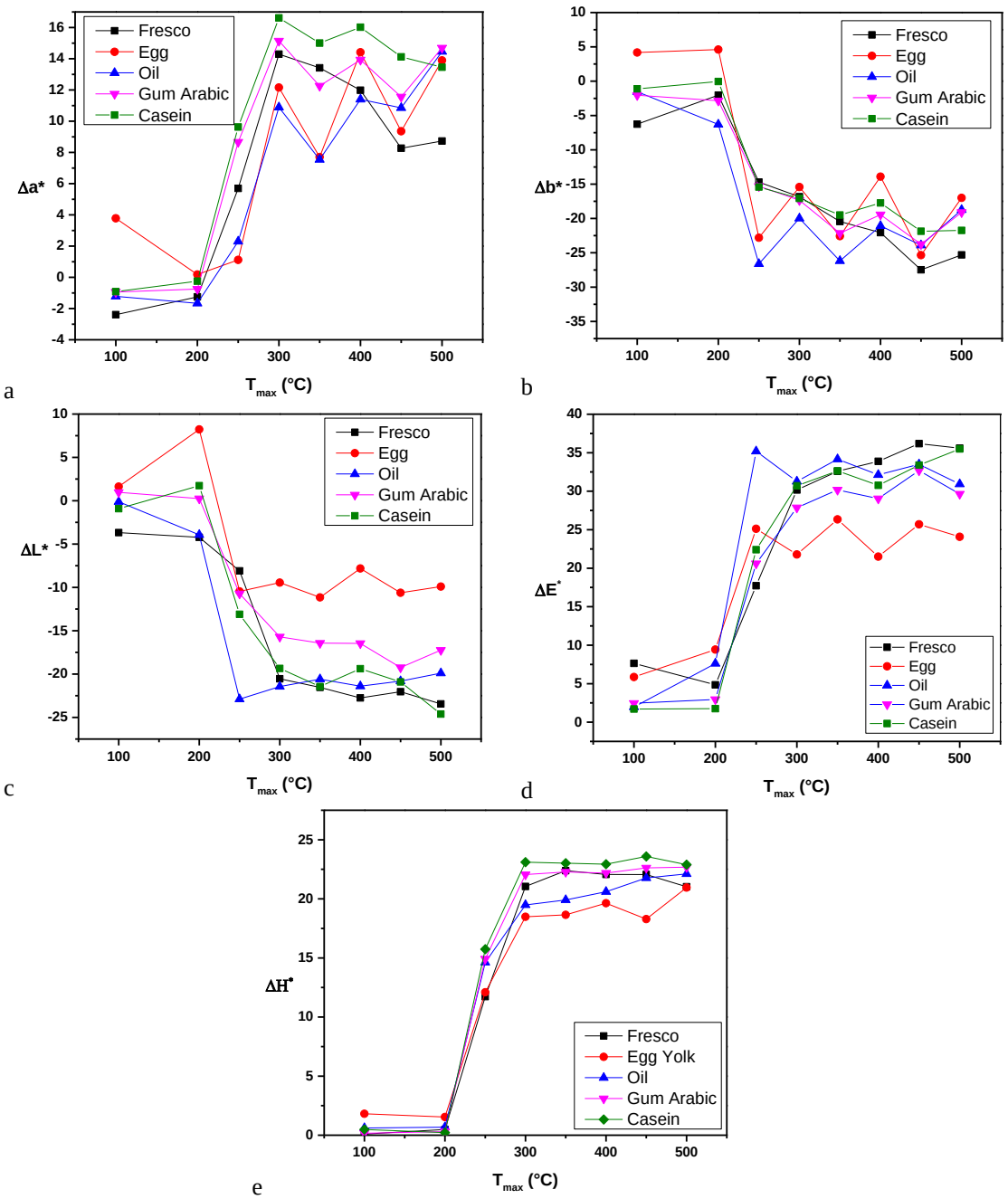

Figure 8: *CIELab color coordinates differences between the painting layer of the initial mock-ups and after the annealing protocol to various T_{max} (a, b and c). Color difference ΔE (d) and hue (e) on the same values.*

4. Conclusions

The present work acts as a preliminary step into the annealing degradation investigation of binding media, that are commonly used in the painting layers of wall paintings. To this direction,

wall painting mock-ups were prepared under the *fresco* and the *secco* wall painting techniques. Painting layers were composed by yellow ochre, while the applied binding media for the *secco* technique were egg yolk, linseed oil, gum Arabic and casein.

FTIR analysis showed that aragonite and $Ca(OH)_2$ are both present in the plaster -together with calcite- even 5 years after its preparation. The difficulty of identifying yellow ochre through FTIR analysis is noted, while goethite is detected with a low participation using XRD. At the same time, TGA analysis was able to distinguish between goethite and lepidocrocite; both these phases were present in the yellow ochre pigment, while goethite was the dominant one.

Yellow ochre's thermal degradation was followed by XRD; goethite starts to transform to hematite below ~300 °C. Kaolinite starts to transform at temperatures above 400 °C; its derivatives could not be discriminated because of their amorphous state. Finally, calcite's transformation to CaO ends before 700 °C. The temperature differentiation between the temperatures of TGA transformations of kaolinite, goethite and calcite and that of XRD is certainly attributed to the annealing protocol itself, as the specimens were kept for 6 h for every T_{max}. The pigment's analysis shows that yellow ochre can be used as a marker over identifying the T_{max} during a fire, as FeOOH transforms to Fe_2O_3 at about 250-300 °C.

Although first color changes started after the annealing protocol at 200 °C for the pigment, as at this temperature it starts getting a warmer hue, the painting layer of the mock-ups is color stable at this temperature, while it presents a dramatical change from and above 250 °C. In all of the cases, the differences observed to the painting layers of the mock-ups -and the pigment itself- are in accordance to the transition of FeOOH to Fe_2O_3. Finally, the macroscopically observed cracks of the plaster start to appear in all the mock-ups under study from $T_{max} \geq 400$ °C, while, for temperatures of 500-600 °C, the mock-ups presented severe splitting, and above this temperature, the mock-ups totally collapsed. This observation leads to the conclusion that -according to the applied fire protocol for compartment fires- the upper limit is set between 400 and 500 °C in terms of plaster's, and consequently of wall painting's integrity. As a future work, the mock-ups prepared under the secco technique should be examined, to determine the existence of binding media degradation residues up to this temperature limit.

Acknowledgments

This work was supported during the Ph.D. research of the corresponding author by the General Secretariat for Research and Technology (GSRT) and the Hellenic Foundation for Research and Innovation (HFRI) (Fellowship Number: 22).

References

[1] J. Romero-Pastor, C. Cardell, Á. Yebra-Rodríguez, A.B. Rodríguez-Navarro, *Validating chemical and structural changes in painting materials by principal component analysis of spectroscopic data using internal mineral standards*, J. Cult. Herit. 14 (2013) 509–514 [doi:10.1016/j.culher.2012.11.006].

[2] M. Gomez-Heras, S. McCabe, B.J. Smith, R. Fort, *Impacts of fire on stone-built Heritage: An overview*, J. Archit. Conserv. 15 (2009) 47–58 [doi:10.1080/13556207.2009.10785047].

[3] T.T. Lie, *Characteristic temperature curves for various fire severities*, Fire Technol. 10 (1974) 315–326 [doi:10.1007/BF02589990].

[4] W.D. Walton, P.H. Thomas, *Estimating Temperatures in Compartment Fires*, in: SFPE Handb. Fire Prot. Eng., Springer New York, New York, NY, 2016: pp. 996–1023

[doi:10.1007/978-1-4939-2565-0_30].
[5] K. Harrison, *The application of forensic fire investigation techniques in the archaeological record*, J. Archaeol. Sci. 40 (2013) 955–959 [doi:10.1016/j.jas.2012.08.030].
[6] T. Uygunoğlu, S. Özgüven, M. Çalış, *Effect of plaster thickness on performance of external thermal insulation cladding systems (ETICS) in buildings*, Constr. Build. Mater. 122 (2016) 496–504. doi:10.1016/j.conbuildmat.2016.06.128.
[7] N. Payraudeau - Le Roux, S. Meille, J. Chevalier, E. Maire, J. Adrien, *In situ observation of plaster microstructure evolution during thermal loading*, Fire Mater. (2016) [doi:10.1002/fam.2357].
[8] A.H. Mostefa, Y. Ghernouti, Y. Sebaibi, *Effectiveness of cement and plaster layers in protection of FRP confined concrete exposed to high temperatures*, J. Adhes. Sci. Technol. 29 (2015) 839–860 [doi:10.1080/01694243.2015.1005860].
[9] M. Hajpál, Á. Török, *Mineralogical and colour changes of quartz sandstones by heat*, in: Environ. Geol., Springer, 2004: pp. 311–322 [doi:10.1007/s00254-004-1034-z].
[10] M. Hajpál, *Fire Damaged Stone Structures in Historical Monuments. Laboratory Analyses of Changes in Natural Stones by Heat Effect*, Building. (2010) 164–173.
[11] O. Sundström, S. Gustavsson, *Simple temperature calculation models for compartment fires*, Luleå University of Technology, 2012.
[12] A. Dionísio, M.A. Sequeira Braga, J.C. Waerenborgh, *Clay minerals and iron oxides-oxyhydroxides as fingerprints of firing effects in a limestone monument*, Appl. Clay Sci. 42 (2009) 629–638 [doi:10.1016/j.clay.2008.05.003].
[13] E. Martinho, A. Dionísio, *Assessment Techniques for Studying the Effects of Fire on Stone Materials: A Literature Review*, Int. J. Archit. Herit. 14 (2020) 275–299 [doi:10.1080/15583058.2018.1535008].
[14] I. Kakoulli, *Late Classical and Hellenistic painting techniques and materials: a review of the technical literature*, Stud. Conserv. 47 (2002) 56–67 [doi:10.1179/sic.2002.47.supplement-1.56].
[15] L. Regazzoni, G. Cavallo, D. Biondelli, J. Gilardi, *Microscopic Analysis of Wall Painting Techniques: Laboratory Replicas and Romanesque Case Studies in Southern Switzerland*, Stud. Conserv. (2018) 1–16 [doi:10.1080/00393630.2017.1422891].
[16] F. Casadio, I. Giangualano, F. Piqué, *Organic materials in wall paintings: the historical and analytical literature*, Stud. Conserv. 49 (2004) 63–80 [doi:10.1179/sic.2004.49.supplement-1.63].
[17] French Ochre JTCLES, Kremer Pigment. GmbH Co.KG. (2020). https://www.kremer-pigmente.com/en/pigments/earth-pigments/1247/french-ochre-jtcles (accessed April 20, 2020).
[18] M. Földvári, *Handbook of the thermogravimetric system of minerals and its use in geological practice*, The Geological Institute of Hungary, Budapest, 2011 [doi:10.1556/CEuGeol.56.2013.4.6].
[19] JCPDS-ICDD, PC Powder Diffraction Files, (2003).
[20] Colorimetry - Part 4: CIE 1976 L*a*b* Colour space, BSi British Standards, 2011.
[21] L. Malletzidou, T.T. Zorba, D. Patsiaoura, D. Lampakis, P. Beinas, V. Touli, K. Chrissafis, I. Karapanagiotis, E. Pavlidou, K.M. Paraskevopoulos, *Unraveling the materials and techniques of post-Byzantine wall paintings: Is there a sole pictorial phase at the catholicon of Stomion, Central Greece?*, Spectrochim. Acta Part A Mol. Biomol. Spectrosc. 206 (2019) 328–339 [doi:10.1016/J.SAA.2018.07.105].
[22] C. Perdikouri, A. Kasioptas, T. Geisler, B.C. Schmidt, A. Putnis, *Experimental study of the aragonite to calcite transition in aqueous solution*, Geochim. Cosmochim. Acta. 75 (2011) 6211–6224 [doi:10.1016/j.gca.2011.07.045].
[23] M.B. Toffolo, E. Boaretto, *Nucleation of aragonite upon carbonation of calcium oxide and calcium hydroxide at ambient temperatures and pressures: a new indicator of fire-related human activities*, J. Archaeol. Sci. 49 (2014) 237–248 [doi:10.1016/J.JAS.2014.05.020].
[24] R.I. Curl, *The Aragonite-Calcite Problem*, NSS Bull. 24 (1962) 57–75.
[25] N. Oriols, N. Salvadó, T. Pradell, S. Butí, *Amorphous calcium carbonate (ACC) in fresco mural paintings*, Microchem. J. 154 (2020) 104567

[doi:10.1016/j.microc.2019.104567].
[26] N. V. Chukanov, I*nfrared spectra of mineral species*, Springer Netherlands, 2014 [doi:https://doi.org/10.1007/978-94-007-7128-4].
[27] Y. Ryskin, *The vibrations of protons in minerals: hydroxyl, water and ammonium*, in: V.C. Farmer (Ed.), Infrared Spectra Miner., Mineralogical Society, London, 1974: pp. 137–181.
[28] V.C. Farmer, *The layer silicates*, in: V.C. Farmer (Ed.), Infrared Spectra Miner., Mineralogical Society, London, 1974: pp. 331–363.
[29] W.B. White, *The carbonate minerals*, in: V.C. Farmer (Ed.), Infrared Spectra Miner., Mineralogical Society, London, 1974.
[30] S. Gunasekaran, G. Anbalagan, S. Pandi, *Raman and infrared spectra of carbonates of calcite structure*, J. Raman Spectrosc. 37 (2006) 892–899 [doi:10.1002/jrs.1518].
[31] M. Anastasiou, T. Hasapis, T. Zorba, E. Pavlidou, K. Chrissafis, K.M. Paraskevopoulos, *TG-DTA and FTIR analyses of plasters from byzantine monuments in Balkan region*, J. Therm. Anal. Calorim. 84 (2006) 27–32 [doi:10.1007/s10973-005-7211-9].
[32] P.S. Thomas, B.H. Stuart, N. McGowan, J.P. Guerbois, M. Berkahn, V. Daniel, *A study of ochres from an Australian aboriginal bark painting using thermal methods*, J. Therm. Anal. Calorim. 104 (2011) 507–513 [doi:10.1007/s10973-011-1336-9].
[33] M. Irfan Khan, H.U. Khan, K. Azizli, S. Sufian, Z. Man, A.A. Siyal, N. Muhammad, M. Faiz ur Rehman, *The pyrolysis kinetics of the conversion of Malaysian kaolin to metakaolin*, Appl. Clay Sci. 146 (2017) 152–161 [doi:10.1016/j.clay.2017.05.017].
[34] C. Genestar Juliá, C. Pons Bonafé, *The use of natural earths in picture: study and differentiation by thermal analysis*, Thermochim. Acta. 413 (2004) 185–192 [doi:10.1016/J.TCA.2003.10.016].
[35] C. Genestar, C. Pons, *Earth pigments in painting: Characterisation and differentiation by means of FTIR spectroscopy and SEM-EDS microanalysis*, Anal. Bioanal. Chem. 382 (2005) 269–274 [doi:10.1007/s00216-005-3085-8].
[36] D. Bikiaris, Sister_Daniilia, S. Sotiropoulou, O. Katsimbiri, E. Pavlidou, A.P. Moutsatsou, Y. Chryssoulakis, *Ochre-differentiation through micro-Raman and micro-FTIR spectroscopies: Application on wall paintings at Meteora and Mount Athos*, Greece, Spectrochim. Acta - Part A Mol. Biomol. Spectrosc. 56 (2000) 3–18 [doi:10.1016/S1386-1425(99)00134-1].